Radioactive decay of $^{288-296}$Og via heavy cluster emission within a modified generalized liquid drop model with a Q-value-dependent preformation factor

K. P. Santhosh ,[*] Tinu Ann Jose, and N. K. Deepak

School of Pure and Applied Physics, Kannur University, Swami Anandatheertha Campus, Payyanur 670327, Kerala, India

A systematic study on radioactive decay of various isotopes of superheavy element oganesson ($Z = 118$) with mass numbers varying from 288 to 296 via heavy cluster emission is considered. The half-life of an emitted cluster is computed using the modified generalized liquid drop model with the Q value dependent preformation factor, for all possible splitting of each Og isotope. The heavy clusters with half-lives comparable to or less than the alpha half-life are probable for emission. From calculations, it is evident that for each Og isotope, the cluster emission with half-life comparable to alpha decay are indium and cadmium, which have nearly a proton magic number ($Z = 50$) and also the cluster emission with minimum half-lives among all splitting are ^{136}Xe and ^{138}Ba, both having a magic neutron number $N = 82$. The role of the magic number in the stability of heavy cluster decay is evident. Modes of decay of each isotope of Og is identified by comparing $T_{1/2}^\alpha$ values with corresponding $T_{1/2}^{\mathrm{SF}}$ values computed using the new mass inertia (I_{rigid}) dependent formula. The experimental alpha decay half-life of ^{294}Og is 0.89 ms and the theoretically predicted value using our model is 0.395 ms. We were able to reproduce experimental alpha decay half-lives and decay modes in the case of ^{294}Og, thereby proving the reliability of our model, hence we believe that the predictions made in the case of other isotopes of Og would serve as a guiding tool for future studies in this field.

I. INTRODUCTION

Research on the superheavy nucleus (SHN) has become one of the important topics in nuclear physics, after the prediction of the island of stability around $Z = 126$ and $N = 184$. Hot fusion reaction [1] and cold fusion reaction [2] techniques are used to synthesize SHN and so far SHN up to $Z = 118$ has been experimentally synthesized. Many attempts to synthesize superheavy nuclei with $Z = 119$ and 120 are being done using evaporation techniques [3,4]. These experimental investigations along with theoretical justification has made this topic a demanding one in the last few years.

Superheavy nuclei with atomic number $Z = 118$ is an element of great interest among researchers since the early 21st century due to its electronic configuration or shell structure. Haba [5] clearly shows the position of oganesson ($Z = 118$) in the periodic table in the seventh row below inert gases. Several theoretical calculations to synthesize SHN were performed by scientists like the fusion-by-diffusion (FBD) model [6–12], the nuclear collectivization model [13,14], and the dinuclear system (DNS) model [15–21]. Many experiments were also conducted to synthesize this element and, finally, Ognessian *et al.* [22] were successful in synthesizing an isotope of Og, the heaviest SHN synthesized so far. A decay chain of SHN Og with $Z = 118$ was discovered for the first time in 2002 at DGFRS [22] in the reaction ^{249}Cf(^{48}Ca, $3n$)^{294}118. Later two more decay chains of ^{294}Og were reported in 2005 [22].

The decay properties of daughter nucleus (^{286}Fl and ^{282}Cn) in the decay chain of ^{294}Og were also confirmed experimentally [23,24]. The prediction of an island of stability in the vicinity of a highly neutron rich domain with $N > 170$ around a magic number, together with these experimental evidence near $Z = 118$, encourages researchers to make extensive study on the synthesis and decay of various isotopes of oganesson.

Just like the works done to synthesize oganesson, several investigations were conducted to study its decay both by the means of calculations and observations. Sobiczewski [25] has theoretically predicted the alpha decay chain of ^{296}Og which is the heaviest nuclide observed in terms of proton and neutron number. Sahayi *et al.* [26] predicted alpha decay half-lives of 22 isotopes of Og with mass numbers ranging from 279 to 300. Bao *et al.* [27] have predicted the decay chain of the nuclei $^{293,295-297}$Og employing generalized liquid drop model (GLDM) and Royer's analytical formula. Ismail *et al.* [28] have theoretically predicted α-decay chains of Og isotopes with mass numbers ranging 290–298, using a realistic nucleon-nucleon interaction. ^{294}Og is the isotope of Og for which the modes of decay and half-life are experimentally known and the properties like structure, decay modes, and half-lives of other isotopes with $Z = 118$ are unknown. To verify the proposed model, researchers have compared the predicted half-life values with the experimentally available values of ^{294}Og.

Generally, SHN decays by alpha emission chain followed by spontaneous fission and the reliable technique to understand newly synthesized SHN is to check the mode by which it

*drkpsanthosh@gmail.com

decays. Alpha decay observation serves as a significant factor to understand the exact information of the initial nucleus in the decay chain. In 1928, Gamow [29] and then independently by Gurney and Condon [30] proposed the concept of alpha decay. Regardless of minor modifications, Gamow theory is used even today to study alpha decay. Several theoretical models are proposed to study the process of alpha decay such as the fission model [31], the cluster model [32], the GLDM [33], and UMADAC [34]. In our present work, alpha decay is studied in the framework of the modified generalized liquid drop model (MGLDM) [35]. The process of spontaneous fission (SF) was proposed by Bohr and Wheeler [36] in 1939, based on the liquid drop model of atomic nuclei.

Modes of decay of SH elements are predicted by comparing alpha decay half-lives predicted by our model with SF half-lives proposed by Bao *et al.* [37] and also with a new mass inertia dependent formula for SF. In the proposed work, we studied the properties of the SH element, oganesson (Og) using the MGLDM with the Q value dependent preformation factor. The Modified generalized liquid drop model (MGLDM) is the modified version of the GLDM incorporating the nuclear proximity potential of Blocki *et al.* [38]. We have calculated the half-life for all possible cluster emissions from various isotopes of the element Og ($Z = 118$) and also the theoretical predictions on the modes of decay are done within the MGLDM with Q dependent preformation factor.

II. MODIFIED GENERALIZED LIQUID DROP MODEL (MGLDM)

In the MGLDM, for a deformed nucleus, the macroscopic energy is defined as

$$E = E_V + E_S + E_C + E_R + E_P. \tag{1}$$

Here the terms E_V, E_S, E_C, E_R, and E_P represent the volume, surface, Coulomb, rotational, and proximity energy terms respectively.

For the prescission region the volume, surface, and Coulomb energies in MeV are given by

$$E_V = -15.494(1 - 1.8I^2)A, \tag{2}$$

$$E_S = 17.9439(1 - 2.6I^2)A^{2/3}\left(S/4\pi R_0^2\right), \tag{3}$$

$$E_C = 0.6e^2(Z^2/R_0) \times 0.5 \int [V(\theta)/V_0][R(\theta)/R_0]^3 \sin\theta d\theta. \tag{4}$$

Here I is the relative neutron excess and S is the surface of the deformed nucleus, $V(\theta)$ is the electrostatic potential at the surface, and V_0 is the surface potential of the sphere.

For the postscission region,

$$E_V = -15.494\left[\left(1 - 1.8I_1^2\right)A_1 + \left(1 - 1.8I_2^2\right)A_2\right], \tag{5}$$

$$E_S = 17.9439\left[\left(1 - 2.6I_1^2\right)A_1^{2/3} + \left(1 - 2.6I_2^2\right)A_2^{2/3}\right], \tag{6}$$

$$E_C = \frac{0.6e^2Z_1^2}{R_1} + \frac{0.6e^2Z_2^2}{R_2} + \frac{e^2Z_1Z_2}{r}. \tag{7}$$

Here A_i, Z_i, R_i, and I_i are the masses, charges, radii, and relative neutron excess of the fragments, r is the distance between the centers of the fragments.

The nuclear proximity potential E_P is given by Blocki *et al.* [38] as

$$E_p(z) = 4\pi\gamma b\left[\frac{C_1C_2}{(C_1 + C_2)}\right]\Phi\left(\frac{z}{b}\right), \tag{8}$$

with the nuclear surface tension coefficient

$$\gamma = 0.9517[1 - 1.7826(N - Z)^2/A^2] \text{ MeV/fm}^2, \tag{9}$$

where N, Z, and A represent neutron, proton, and mass number of the parent nucleus respectively, Φ represents the universal proximity potential [39] given as

$$\Phi(\varepsilon) = -4.41e^{-\varepsilon/0.7176}, \quad \text{for } \varepsilon > 1.9475, \tag{10}$$

$$\Phi(\varepsilon) = -1.7817 + 0.9270\varepsilon + 0.01696\varepsilon^2 - 0.05148\varepsilon^3,$$
$$\text{for} \quad 0 \leqslant \varepsilon \leqslant 1.9475, \tag{11}$$

with $\varepsilon = z/b$, where the width (diffuseness) of the nuclear surface is $b \approx 1$ fm and the Süsmann central radii C_i of fragments related to sharp radii R_i is

$$C_i = R_i - \left(\frac{b^2}{R_i}\right). \tag{12}$$

For R_i we use the semiempirical formula in terms of mass number A_i as [39]

$$R_i = 1.28A_i^{1/3} - 0.76 + 0.8A_i^{-1/3}. \tag{13}$$

The barrier penetrability P is calculated using

$$P = \exp\left\{-\frac{2}{\hbar}\int_{R_{in}}^{R_{out}}\sqrt{2B(r)[E(r) - E(\text{sphere})]}dr\right\}, \tag{14}$$

where $R_{in} = R_1 + R_2$, $B(r) = \mu$ and $R_{out} = e^2Z_1Z_2/Q$. R_1 and R_2 are the radius of the daughter nuclei and emitted cluster respectively, μ is the reduced mass, and Q is the released energy.

The partial half-life is related to the decay constant λ by

$$T_{1/2} = \left(\frac{\ln 2}{\lambda}\right) = \left(\frac{\ln 2}{\nu P_C P}\right). \tag{15}$$

The assault frequency ν has been taken as 10^{20} s^{-1} and the preformation factor [35] is given as

$$P_C = 10^{aQ+bQ^2+c}, \tag{16}$$

with $a = -0.25736$, $b = 6.37291 \times 10^{-4}$, $c = 3.35106$, and Q is the Q value or the energy released in a radioactive nuclear reaction.

III. RESULTS AND DISCUSSION

Half-lives of radioactive decay of various isotopes of SHN Og with mass numbers varying from 288 to 296 via heavy cluster emission are done using the MGLDM with Q value

dependent preformation factor. We know that the most radioactive nucleus with Z greater than 100 is unstable due to high proton-proton repulsion. But the mere prediction of stability of the magic number due to the shell effect has motivated researchers to predict an island of stability near the superheavy region. The experimental discovery of certain isotopes in a superheavy region like ^{294}Og serve as simple evidence to this prediction of stable nuclei near the island of stability. We could experimentally synthesize other heavier isotopes of Og easily if we knew the predicted range of experimental observables beforehand like half-life, energy, etc., so that we can design our experimental setup accordingly. Therefore good theoretical studies, where the predictions go hand in hand with experiments, are essential for the better understanding of superheavy nuclei. In our present work, half-lives are calculated using the MGLDM with Q dependent preformation factor. The MGLDM, or modified generalized liquid drop model, is a well proved theoretical model by Santhosh *et al.* [35] where the GLDM of Royer [40,41] is modified by adding a proximity potential developed by Blocki *et al.* [38],

$$Q = \Delta M_p - (\Delta M_d + \Delta M_c), \tag{17}$$

representing the decay energy or Q value of the reaction, where ΔM_p, ΔM_d, and ΔM_c are the masses of parent, daughter nuclei and cluster respectively. The masses are taken from Ref. [42] and those nuclei whose experimental values are not available are taken from KTUY05 [43].

In our present work to understand the properties of SHN, $Z = 118$ with mass number ranging 288–296, we have considered all cluster daughter combinations possible using the concept of the cold reaction valley plot, which was presented in relation to the minima in the driving potential. The driving potential is generally defined as the difference between the interaction potential (V) and decay energy (Q value) of the reaction process. The driving potential ($V - Q$) for the parent nucleus is calculated for all possible fragments as a function of charge and mass asymmetries. For every fixed mass pair (A_1, A_2), a pair of charges (Z_1, Z_2) is pointed out for which the driving potential is a minimum in the calculated fragmentation potential. Then for the calculated fragment combination, half-lives are computed within the MGLDM and also calculated the branching ratio, for all possible heavy cluster emissions of each Og isotope. By using the presently available technique [44], i.e., by using solid state nuclear track detectors (SS-NTDs), a cluster decay half-life up to 10^{30} s and a branching ratio down to 10^{-19} can be measured. The branching ratio is calculated using the formula

$$b = \frac{\lambda_{\text{cluster}}}{\lambda_\alpha} = \frac{T_{1/2}^\alpha}{T_{1/2}^{\text{cluster}}}, \tag{18}$$

where λ_{cluster} and λ_α are the decay constant corresponding to cluster emission and alpha decay from parent superheavy nuclei. $T_{1/2}^\alpha$ is the alpha decay half-life and $T_{1/2}^{\text{cluster}}$ is the cluster decay half-life.

Figure 1 shows the variation of the logarithm of half-life drawn along the Y axis with respect to cluster size on the X axis for all splitting in the case of ^{291}Og. Note that the frag-
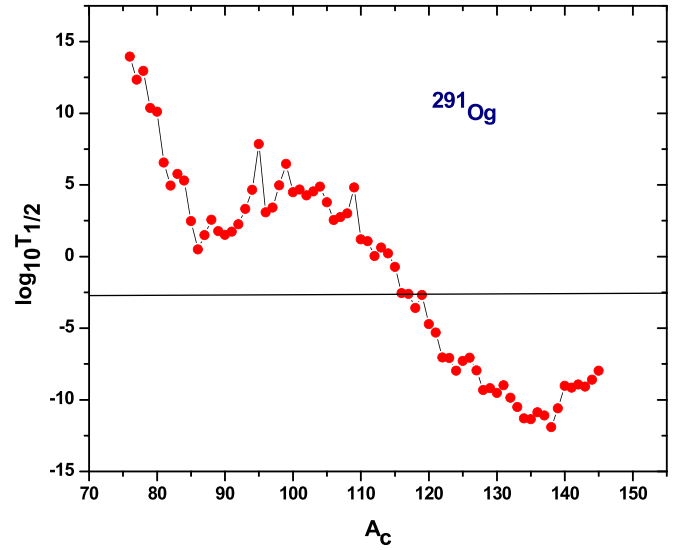

FIG. 1. Graph showing the variation of logarithm of half-life vs cluster size for the isotope of ^{291}Og. Horizontal line represents the alpha half-life. Half-lives are in seconds.

ment combination in Fig. 1 represents the minima in the cold reaction valley plot of ^{291}Og. From the graph it is clear that as cluster size increases, the half-life shows a zigzag decreasing pattern, reaches a minimum value, and then increases. The straight line plotted in the figure corresponds to the logarithm of alpha decay half-life in the case of ^{291}Og. In the case of all other isotopes of Og similar graphs are drawn and the graph corresponding to $^{292-295}$Og is shown in Fig. 2. The fragment combinations in Fig. 2 also represent the minima in the cold reaction valley of $^{292-295}$Og respectively. In the half-life versus cluster size plot, there are few peaks and dips for which the half-life shows a high or low value compared to nearby fragment combinations. In the case of ^{291}Og, [^{86}Kr($N = 50$) + ^{205}Pb($Z = 82$)], [^{112}Pd($Z = 46$) + ^{179}Hf], [^{118}Cd($Z = 48$) + ^{173}Yb], and [^{124}Sn($Z = 50$) + ^{167}Er] are the fragment combinations that show a small dip in half-life compared to their neighbors and [^{138}Ba($N = 82$) + ^{153}Sm] is the combination with least half-life. The shell structure reveals that either one or both fragments in the dip have a magic number of proton or neutron or near it. All the graphs in Figs. 1 and 2 shows a similar pattern and there are cluster emissions from each parent Og nucleus for which the half-life is comparable to that of alpha decay and also the cluster emission with minimum decay half-life. It should be noted that the heavy clusters with half-lives comparable to or less than the alpha half-life are probable for emission.

Among all possible chances of cluster decay from each isotope of Og, with mass numbers ranging 288–296, the probable cluster emissions with half-life in the range 10^{-8}–100 s, which are sufficient to detect them in the laboratory, are listed in Table I. The parent nuclei are given in column 1. The logarithm of cluster decay half-life and branching ratio calculated using our model shown in the fifth and seventh columns is compared with the values by Poenaru *et al.* [45], shown in the sixth and eighth columns. In the case of each Og isotope,
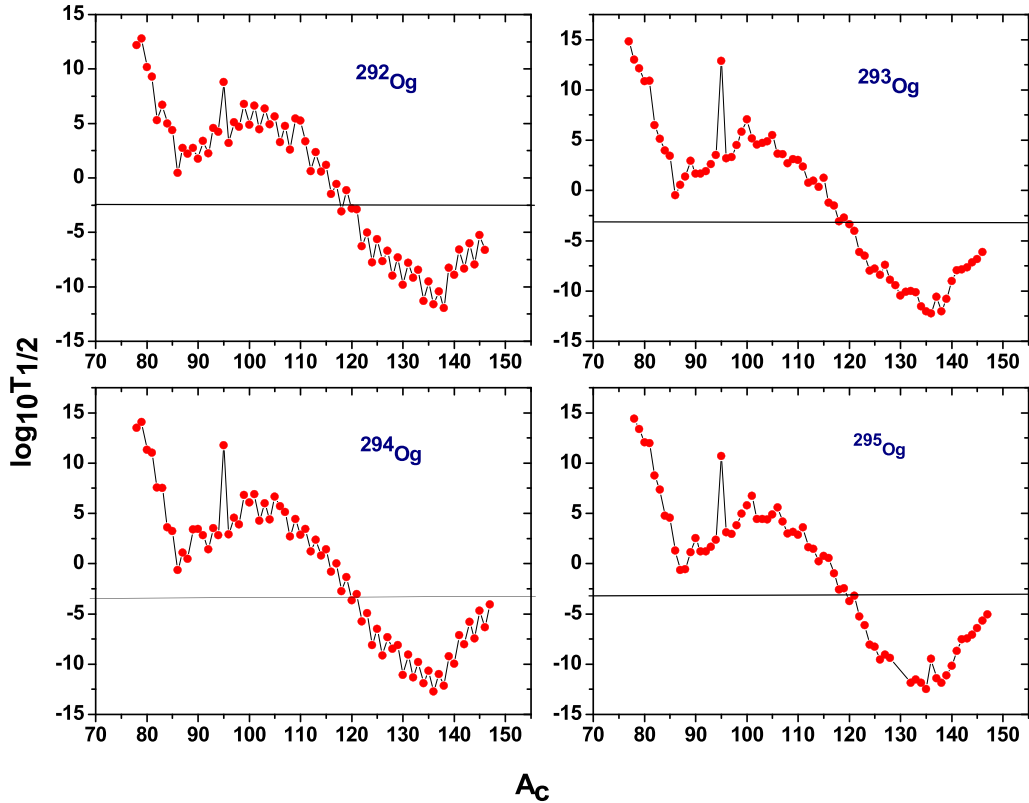
FIG. 2. Graph shows the variation of logarithm of half-life vs cluster size for various isotopes of Og from 292 to 295. Horizontal lines represent the alpha half-lives. Half-lives are in seconds.

the alpha decay half-life is given in the first row following the parent isotope and the other probable heavy clusters are given below. Based on the half-life calculated, we predict which decay chances are probable. One of the usual signs of cluster decay is that the mass of the daughter nucleus will be greater than the cluster fragments. In some cases, we got a fragment combination having similar proton numbers like various isotopes of Ce ($Z = 58$) and Nd ($Z = 60$) in the case of $^{291-296}$Og with a half-life in the range $10^{-8}-100$ s. As it is inappropriate to have cluster decay with similar masses, we neglected fragments with a similar proton number as the cluster decay. The shell closure effect of one or both decay products for fission or cluster radioactivity plays a key role. In Table I, for the parent nuclei, $^{288-296}$Og, it is noteworthy that most of the probable clusters emitted like Cd, Sn, I (with $Z = 50$ or near it) are stable with the magic number of protons and also in other cases the daughter nucleus is Pb ($Z = 82$). The stable nature of these fragments and the half-life predicted in the measurable range assures the chances of several such mentioned decays to occur and to detect them in the near future, once the SHN is synthesized in the laboratory.

As stated earlier, we have calculated half-lives for all possible splitting of each Og isotope within the MGLDM with the Q value dependent preformation factor and then compared it with its alpha decay half-lives. Alpha decay is one of the dominant decay mechanisms in SHN and is crucial in determining many properties of SHN. In many cases the unknown parent nucleus is identified based on its alpha decay. Since SHN decays mainly by alpha decay, chances of other cluster

with a half-life comparable to that of the alpha decay half-life is also probable. Table II denotes the cluster decay with half-lives comparable to that of alpha decay half-lives, for various isotopes of Og parent nucleus, with mass numbers varying from 288 to 296. It is evident from calculations that, for isotopes with even mass numbers $A = 288$, 290, 292, and 294, the probable cluster with half-lives comparable to that of alpha decay half-life is cadmium with $Z = 48$ and indium with $Z = 49$ (both having atomic number close to magic number $Z = 50$) leading to a daughter nucleus of ytterbium and thulium. And for isotopes with odd mass numbers $A = 289$, 291, 293, and 295, probable cluster is found to be different isotopes of cadmium, with ytterbium as the daughter nucleus. In our previous work, the probable clusters emitted in the case of ^{296}Og [46] are found to be krypton with doubly magic lead and palladium with a hafnium daughter nucleus. Generally unstable radioactive parent nucleus decays by alpha or cluster radioactivity and becomes a stable daughter nucleus. In all the decay mechanisms mentioned, one of the decay products has either N or Z as a magic number or very close to it. Through our present work, the role of magic numbers in stability is very clear. We are eagerly waiting to receive experimental information about the SHN, Og, to confirm our predictions. Half-lives of some cluster radioactivity are comparable to alpha decay half-lives, but we have not considered cluster radioactivity in predicting decay modes because cluster radioactivity is a rare process [47,48]. The rare nature of this process stems from the fact that cluster emission is masked by a large number of alpha decay events. For, e.g., Rose and Jones [49] were able

TABLE I. Half-life and branching ratio for various clusters probable from $^{288-296}$Og isotopes.

Parent nuclei	Emitted cluster	Daughter Nuclei	Q value (MeV)	$\log_{10}T_{1/2}$ Present	[44]	$\log_{10}b$ Present	[44]
^{288}Og	^{4}He	^{284}Lv	11.905	−3.46105			
	^{109}Rh	^{179}Ta	333.428	−0.66773		−2.79324	
	^{111}Pd	^{177}Pb	333.943	0.86588		−4.32685	
	^{112}Pd	^{176}Pb	335.638	−0.78772		−2.67325	
	^{113}Ag	^{175}Lu	336.933	−0.01912		−3.44185	
	^{114}Cd	^{174}Yb	341.699	−2.62783		−0.83314	
	^{115}Cd	^{173}Yb	340.376	−1.48799		−1.97298	
	^{116}Cd	^{172}Yb	342.708	−3.80827		0.34730	
	^{117}Cd	^{171}Yb	340.465	−1.75740		−1.70357	
	^{118}Cd	^{170}Yb	342.206	−3.51665		0.05568	
	^{119}In	^{169}Tm	343.714	−3.23063		−0.23034	
	^{120}Sn	^{168}Er	348.830	−6.71527		3.25429	
	^{121}Sn	^{167}Er	347.229	−5.17148		1.71051	
	^{122}Sn	^{166}Er	349.607	−7.75173		4.29076	
	^{123}Sn	^{165}Er	347.078	−5.19112		1.73015	
	^{124}Sn	^{164}Er	348.917	−7.19250		3.73153	
	^{131}I	^{157}Tb	352.946	−7.56221		4.10124	
^{289}Og	^{4}He	^{285}Lv	11.785	−3.20176			
	^{110}Pd	^{179}Pb	334.804	−0.06070		−3.14103	
	^{111}Pd	^{178}Pb	334.431	0.17173		−3.37346	
	^{112}Pd	^{177}Pb	335.213	−0.65462		−2.54712	
	^{113}Pd	^{176}Pb	334.177	0.19835		−3.40008	
	^{114}Cd	^{175}Yb	340.720	−1.97852		−1.22321	
	^{115}Cd	^{174}Yb	341.039	−2.38060		−0.82113	
	^{116}Cd	^{173}Yb	342.274	−3.67428		0.47254	
	^{117}Cd	^{172}Yb	341.684	−3.20048		−0.00125	
	^{118}Cd	^{171}Yb	342.019	−3.62763		0.42589	
	^{119}Sn	^{170}Er	346.184	−4.25737		1.05564	
	^{120}Sn	^{169}Er	348.032	−6.21122		3.00949	
	^{121}Sn	^{168}Er	348.199	−6.48561		3.28387	
	^{122}Sn	^{167}Er	349.243	−7.70769		4.50596	
	^{123}Sn	^{166}Er	348.752	−7.27221		4.07047	
	^{124}Sn	^{165}Er	348.766	−7.38193		4.18020	
	^{125}Sn	^{164}Er	347.849	−6.48233		3.28059	
^{290}Og	^{4}He	^{286}Lv	11.645	−2.88941			
	^{110}Pd	^{180}Pb	333.740	0.65651		−3.54723	
	^{112}Pd	^{178}Pb	334.387	−0.14891		−2.74181	
	^{114}Pd	^{176}Pb	333.697	0.28388		−3.17460	
	^{115}Ag	^{175}Lu	335.779	0.33127		−3.22200	
	^{116}Cd	^{174}Yb	341.287	−2.99916		0.10844	
	^{117}Cd	^{173}Yb	339.600	−1.48945		−1.40126	
	^{118}Cd	^{172}Yb	341.587	−3.49600		0.60528	
	^{119}In	^{171}Tm	342.539	−2.67361		−0.21711	
	^{120}Sn	^{170}Er	346.837	−5.30425		2.41353	
	^{121}Sn	^{169}Er	345.750	−4.31053		1.41981	
	^{122}Sn	^{168}Er	348.563	−7.31487		4.42415	
	^{123}Sn	^{167}Er	346.737	−5.48075		2.59003	
	^{124}Sn	^{166}Er	348.790	−7.76887		4.87815	
	^{131}I	^{159}Tb	352.605	−7.91558		5.02486	
^{291}Og	^{4}He	^{287}Lv	11.595	−2.79048			
	^{86}Kr	^{205}Pb	304.166	0.50122		−3.29038	
	^{112}Pd	^{179}Hf	333.915	0.03158		−2.82074	
	^{113}Pd	^{178}Hf	333.156	0.62595		−3.41511	
	^{114}Pd	^{177}Hf	333.502	0.20744		−2.99660	
	^{115}Cd	^{176}Yb	338.706	−0.73277		−2.05639	
	^{116}Cd	^{175}Yb	340.538	−2.55647		−0.23269	

TABLE I. (*Continued.*)

Parent nuclei	Emitted cluster	Daughter Nuclei	Q value (MeV)	$\log_{10}T_{1/2}$		$\log_{10}b$	
				Present	[44]	Present	[44]
	^{117}Cd	^{174}Yb	340.493	−2.61423		−0.17493	
	^{118}Cd	^{173}Yb	341.383	−3.58701		0.79785	
	^{119}Cd	^{172}Yb	340.365	−2.68393		−0.10523	
	^{120}Sn	^{171}Er	345.947	−4.71406		1.92490	
	^{121}Sn	^{170}Er	346.436	−5.30391		2.51475	
	^{122}Sn	^{169}Er	347.994	−7.04208		4.25292	
	^{123}Sn	^{168}Er	347.937	−7.08221		4.29305	
	^{124}Sn	^{167}Er	348.655	−7.98363		5.19447	
	^{125}Sn	^{166}Er	347.952	−7.29250		4.50334	
	^{126}Sn	^{165}Er	347.667	−7.06700		4.27784	
	^{127}Te	^{164}Dy	351.380	−7.96231		5.17315	
^{292}Og	^{4}He	^{288}Lv	11.465	−2.49349			
	^{86}Kr	^{206}Pb	303.971	0.44487		−2.93865	
	^{112}Pd	^{180}Hf	333.021	0.60168		−3.09546	
	^{114}Pd	^{178}Hf	332.846	0.55799		−3.05177	
	^{116}Cd	^{176}Yb	339.124	−1.48288		−1.01090	
	^{117}Cd	^{175}Yb	338.034	−0.55884		−1.93494	
	^{118}Cd	^{174}Yb	340.567	−3.06950		0.57572	
	^{119}Cd	^{173}Yb	338.451	−1.12847		−1.36531	
	^{120}Cd	^{172}Yb	340.132	−2.83599		0.34221	
	^{121}In	^{171}Tm	341.966	−2.88856		0.39478	
	^{122}Sn	^{170}Er	346.970	−6.27778		3.78401	
	^{123}Sn	^{169}Er	345.659	−5.00738		2.51361	
	^{124}Sn	^{168}Er	348.145	−7.77127		5.27749	
	^{125}Sn	^{167}Er	346.108	−5.64599		3.15221	
	^{126}Sn	^{166}Er	347.861	−7.64679		5.15302	
	^{127}Sb	^{165}Ho	348.518	−6.71117		4.21739	
	^{129}Te	^{163}Dy	350.306	−7.30224		4.80846	
	^{131}I	^{161}Tb	351.824	−7.78839		5.29461	
^{293}Og	^{4}He	^{289}Lv	11.915	−3.56864			
	^{86}Kr	^{207}Pb	304.588	−0.46357		−3.10564	
	^{87}Kr	^{206}Pb	303.365	0.55612		−4.12534	
	^{112}Pd	^{181}Hf	332.595	0.74406		−4.31327	
	^{113}Pd	^{180}Hf	332.240	0.96515		−4.53437	
	^{114}Pd	^{179}Hf	332.824	0.32447		−3.89368	
	^{116}Cd	^{177}Yb	338.569	−1.22554		−2.34368	
	^{117}Cd	^{176}Yb	338.780	−1.52278		−2.04643	
	^{118}Cd	^{175}Yb	340.268	−3.06116		−0.50805	
	^{119}Cd	^{174}Yb	339.795	−2.69539		−0.87382	
	^{120}Cd	^{173}Yb	340.378	−3.37138		−0.19783	
	^{121}Sn	^{172}Er	344.551	−4.01208		0.44286	
	^{122}Sn	^{171}Er	346.530	−6.13819		2.56897	
	^{123}Sn	^{170}Er	346.795	−6.52334		2.95413	
	^{125}Sn	^{168}Er	347.758	−7.79907		4.22986	
	^{127}Sn	^{166}Er	347.267	−7.43160		3.86239	
^{294}Og	^{4}He	^{290}Lv	11.835	−3.40230			
	^{86}Kr	^{208}Pb	304.474	−0.63583	−2.45	−2.76673	−0.87
	^{88}Kr	^{206}Pb	302.937	0.48555		−3.88811	
	^{114}Pd	^{180}Hf	332.730	0.81066		−4.21321	
	^{116}Cd	^{178}Yb	337.867	−0.82897		−2.57358	
	^{117}Cd	^{177}Yb	336.865	0.00865		−3.41120	
	^{118}Cd	^{176}Yb	339.653	−2.73975		−0.66281	
	^{119}Cd	^{175}Yb	338.136	−1.36829		−2.03426	
	^{120}Cd	^{174}Yb	340.362	−3.65040		0.24784	
	^{121}In	^{173}Tm	341.552	−3.03173		−0.37083	
	^{122}Sn	^{172}Er	345.885	−5.77836		2.37581	

TABLE I. (*Continued.*)

Parent nuclei	Emitted cluster	Daughter Nuclei	Q value (MeV)	$\log_{10}T_{1/2}$ Present	[44]	$\log_{10}b$ Present	[44]
	^{123}Sn	^{171}Er	344.995	−4.94784		1.54528	
	^{125}Sn	^{169}Er	346.280	−6.49735		3.09479	
	^{127}Sb	^{167}Ho	348.440	−7.32323		3.92067	
^{295}Og	^{4}He	^{291}Lv	11.695	−3.09366			
	^{87}Kr	^{208}Pb	303.968	−0.64649	0.50	−2.44701	−2.73
	^{88}Kr	^{207}Pb	303.653	−0.58513		−2.50837	
	^{114}Pd	^{181}Hf	332.404	0.20818		−3.30169	
	^{115}Pd	^{180}Hf	331.715	0.74820		−3.84170	
	^{116}Pd	^{179}Hf	331.805	0.56547		−3.65897	
	^{117}Cd	^{178}Yb	337.623	−0.95817		−2.13533	
	^{118}Cd	^{177}Yb	339.198	−2.57305		−0.52045	
	^{119}Cd	^{176}Yb	338.981	−2.46107		−0.63243	
	^{120}Cd	^{175}Yb	340.163	−3.74549		0.65199	
	^{121}Cd	^{174}Yb	339.528	−3.20159		0.10809	
	^{122}Sn	^{173}Er	345.101	−5.27206		2.17856	
	^{123}Sn	^{172}Er	345.810	−6.12456		3.03106	
^{296}Og	^{4}He	^{292}Lv	9.805	1.98803			
	^{88}Kr	^{208}Pb	301.909	1.05243		0.93561	
	^{116}Pd	^{180}Hf	330.081	1.91330		0.07470	
	^{118}Cd	^{178}Yb	336.867	−0.60145		2.58949	
	^{119}Cd	^{177}Yb	335.436	0.64411		1.34393	
	^{120}Cd	^{176}Yb	337.918	−1.79617		3.78421	
	^{121}Cd	^{175}Yb	336.239	−0.27723		2.26527	
	^{122}Cd	^{174}Yb	338.027	−2.08576		4.07379	
	^{123}In	^{173}Tm	340.156	−2.40502		4.39305	
	^{124}Sn	^{172}Er	345.188	−5.88289		7.87093	
	^{125}Sn	^{171}Er	344.085	−4.80916		6.79719	
	^{126}Sn	^{170}Er	346.594	−7.66282		9.65086	
	^{127}Sn	^{169}Er	344.864	−5.81222		7.80026	
	^{129}Sb	^{167}Ho	347.380	−7.02102		9.00906	
	^{131}Te	^{165}Dy	349.294	−7.76680		9.75484	
	^{139}Ba	^{157}Sm	352.062	−7.19434		9.18237	
	^{140}Ba	^{156}Sm	353.099	−8.37587		10.36391	
	^{141}Ba	^{155}Sm	350.394	−5.50001		7.48805	
	^{142}Ba	^{154}Sm	350.767	−5.91077		7.89881	

to detect a few 14-carbon events from ^{223}Ra, within the alpha particle background about 10^9 times higher, using $\Delta E - E$ surface barrier Si detectors.

Table III shows the comparison of the alpha decay half-life of SHN computed using our MGLDM with a Q value dependent preformation factor with the lone experimental data [22] and other theoretical models like VSS, UDL, UNIV, mB1, SemFIS2, and Royer analytical formulas. The phenomenological Viola-Seaborg semiempirical formula (VSS) contains new constants determined by Sobiczewski *et al.* [50,51]. Qi *et al.* [52] proposed the universal decay law (UDL). The universal curve proposed by Poenaru *et al.* [53] is UNIV. The modified Brown (mB1) formula was proposed by Budaca *et al.* [54] with an additional hindrance term depending on parity. "SemFIS2" denotes the semiempirical formula for α-decay half-lives proposed by Poenaru *et al.* [55]. Royer [56] formulated the analytical formulas for α decay. For ^{294}Og, the experimental alpha half-life is 0.89 ms [22] and the the-

oretically predicted value using our model is 0.395 ms. An impressive observation from the table is that the alpha decay half-lives calculated by our formula shows quite good agreement with the experimental half-life as well as with the half-life predicted by other theoretical models. In Table III, our model, UNIV, and UDL show a similar trend in alpha decay half-life, increasing from ^{288}Og, reaching a peak value at ^{292}Og, and decreasing to minima at ^{293}Og and then increasing. Other models, though, do not show any particular trend, but have a peak at ^{291}Og. The peak in the alpha decay half-life corresponds to the stability of the parent nucleus and hence has more of a chance to synthesize them as the existence of the atom is limited by the stability of the nucleus. Therefore, without any doubt, one could tell that our model, the MGLDM with a Q value dependent preformation factor, is a reliable theoretical model to determine cluster decay half-life.

We know that the chances to detect or synthesize SHN in the laboratory are a tedious process due to its decreased

TABLE II. The possible heavy cluster decay from Og parent nuclei with half-life comparable to that of alpha decay half-life.

Parent nuclei	Probable cluster	Daughter nuclei	Q value (MeV)	$T_{1/2}^{cluster}$(s)	$T_{1/2}^{\alpha}$(s)	Branching ratio
^{288}Og	^{116}Cd	^{172}Yb	342.71	1.56×10^{-4}	3.46×10^{-4}	2.22×10^{0}
	^{118}Cd	^{170}Yb	342.21	3.04×10^{-4}		1.14×10^{0}
	^{119}In	^{169}Tm	343.71	5.88×10^{-4}		0.59×10^{0}
^{289}Og	^{116}Cd	^{173}Yb	342.27	2.12×10^{-4}	6.28×10^{-4}	2.97×10^{0}
	^{117}Cd	^{172}Yb	341.68	6.30×10^{-4}		0.99×10^{0}
	^{118}Cd	^{171}Yb	342.02	2.36×10^{-4}		2.67×10^{0}
^{290}Og	^{116}Cd	^{174}Yb	341.29	1.00×10^{-3}	1.29×10^{-3}	1.28×10^{0}
	^{119}In	^{171}Tm	342.54	2.12×10^{-3}		0.61×10^{0}
^{291}Og	^{116}Cd	^{175}Yb	340.54	2.78×10^{-3}	1.62×10^{-3}	5.85×10^{-1}
	^{117}Cd	^{174}Yb	340.49	2.43×10^{-3}		6.68×10^{-1}
	^{119}Cd	^{172}Yb	340.37	2.07×10^{-3}		7.85×10^{-1}
^{292}Og	^{120}Cd	^{172}Yb	340.13	1.46×10^{-3}	3.21×10^{-3}	2.20×10^{0}
	^{121}In	^{171}Tm	341.97	1.29×10^{-3}		2.48×10^{0}
^{293}Og	^{118}Cd	^{175}Yb	340.27	8.69×10^{-4}	2.70×10^{-4}	3.10×10^{-1}
	^{120}Cd	^{173}Yb	340.38	4.25×10^{-4}		6.34×10^{-1}
^{294}Og	^{120}Cd	^{174}Yb	340.36	2.24×10^{-4}	3.96×10^{-4}	1.77×10^{0}
	^{121}In	^{173}Tm	341.55	9.30×10^{-4}		4.26×10^{-1}
^{295}Og	^{120}Cd	^{175}Yb	340.16	1.80×10^{-4}	8.06×10^{-4}	4.49×10^{0}
	^{121}Cd	^{174}Yb	339.53	6.29×10^{-4}		1.28×10^{0}
^{296}Og	^{88}Kr	^{208}Pb	301.91	11.28×10^{0}	97.28×10^{0}	8.62×10^{0}
	^{116}Pd	^{180}Hf	330.08	81.90×10^{0}		1.19×10^{0}

stability against fission. As we progress to synthesize heavier elements, lifetimes tend to get shorter and if synthesized, there is a high chance for it to decay to stable fragments immediately by various modes of decay. There are cases where heavy particle emissions are stronger than alpha decay. Concepts of heavy particle radioactivity (HPR) permit the spontaneous emission of the heavy particle with a larger atomic number, $Z_C > 28$ from SHN with $Z > 110$ [45,57,58]. Most probably when an unstable parent nucleus undergoes spontaneous fission, then the corresponding daughter nucleus will be highly stable with the least half-life. Thus one can predict that in the case of superheavy nuclei the chances of cluster decay with minimum half-life will be most probable to occur and hence should be close to a magic number. In our present work, we have noted the heavy cluster decay with minimum half-life among all splitting of each Og isotope. The most probable

cluster with minimum half-life, daughter nucleus, and the calculated half-lives are given in Table IV. It is quite interesting that in the cases of $^{288-291}$Og, the most probable heavy cluster emitted with minimum half-life is ^{138}Ba ($N = 82$) with different isotopes of Sm daughter nucleus. In the case of ^{292}Og and ^{294}Og, both ^{136}Xe ($N = 82$) and ^{138}Ba are the most probable heavy cluster emitted with minimum half-life. Similarly, in the case of ^{293}Og, ^{295}Og, and ^{296}Og [46], ^{136}Xe is the emitted cluster with the least half-life. It is noteworthy that both predicted most probable clusters, ^{138}Ba and ^{136}Xe, have the neutron number $N = 82$. A minimum in half-life corresponds to greater barrier penetrability which in turn indicates a high chance for such decay to occur. The most stable and favorable fragment combination possible for each unstable parent Og isotope is found for fragment combinations with the deepest minimum half-life in the graphs in Figs. 1 and 2 due to the

TABLE III. Comparison of alpha decay half-life from parent nuclei $^{288-296}$Og using our model with various theoretical models and also with experimental data.

Parent nuclei	Q value (MeV)	$T_{1/2}^{\alpha}$(s)						
		Present model	Expt. [22]	VSS [46,47]	UDL [48]	UNIV [49]	mB1 [50]	SemFIS2 [51]	Royer [52]
^{288}Og	11.9051	0.00035		0.00039	0.00033	0.00016	0.00039	0.00084	0.00030
^{289}Og	11.7851	0.00063		0.00848	0.00062	0.00028	0.00196	0.00672	0.00312
^{290}Og	11.6451	0.00129		0.00155	0.00134	0.00056	0.00124	0.00326	0.00111
^{291}Og	11.5951	0.00162		0.02367	0.00172	0.00070	0.00454	0.01747	0.00800
^{292}Og	11.4651	0.00321		0.00416	0.00354	0.00134	0.00278	0.00787	0.00274
^{293}Og	11.9151	0.00027		0.00426	0.00026	0.00013	0.00112	0.00276	0.00134
^{294}Og	11.8351	0.00040	0.00089	0.00056	0.00039	0.00018	0.00054	0.00089	0.00034
^{295}Og	11.6951	0.00081		0.01374	0.00084	0.00036	0.00291	0.00707	0.00397
^{296}Og	9.8051	97.28080		133.51500	182.8666	26.68844	13.57613	166.2769	72.56321

TABLE IV. The most probable heavy cluster decay from Og parent nuclei with least half-life among all splitting.

Parent nuclei	Most probable cluster	Daughter nuclei	Q value (MeV)	$T_{1/2}^{\text{cluster}}$(s)	Branching ratio
^{288}Og	^{138}Ba	^{150}Sm	360.05	1.20×10^{-13}	2.81×10^{9}
^{289}Og	^{138}Ba	^{151}Sm	358.85	3.37×10^{-13}	7.50×10^{8}
^{290}Og	^{138}Ba	^{152}Sm	358.65	5.35×10^{-13}	2.40×10^{9}
^{291}Og	^{138}Ba	^{153}Sm	357.95	1.24×10^{-12}	1.31×10^{9}
^{292}Og	^{136}Xe	^{156}Gd	355.88	2.40×10^{-12}	1.33×10^{9}
	^{138}Ba	^{154}Sm	357.64	1.08×10^{-12}	2.96×10^{9}
^{293}Og	^{136}Xe	^{157}Gd	356.12	5.87×10^{-13}	4.59×10^{8}
^{294}Og	^{138}Ba	^{156}Sm	357.08	7.12×10^{-13}	5.56×10^{8}
	^{136}Xe	^{158}Gd	356.58	1.87×10^{-13}	2.12×10^{9}
^{295}Og	^{135}Xe	^{160}Gd	355.86	3.31×10^{-13}	2.43×10^{9}
^{296}Og	^{136}Xe	^{160}Gd	354.84	9.96×10^{-13}	9.76×10^{13}

presence of the neutron magic number. Thus the role of a magic number in stability is again evident from this study.

The main decay mechanism observed in SHN is the alpha decay followed by spontaneous fission (SF). A detailed study on alpha decay chains in SHN helps in the identification of new nuclides. One of the experimentally measurable quantities in the alpha decay chain of SHN is its half-life. So in order to check the correctness of a theoretical model, we calculate the alpha decay half-life using that model and then compare it with experimental values. To calculate decay modes, alpha decay half-lives are computed using the MGLDM and SF half-lives are determined using the following formula of Bao *et al.* [37]:

$$\log_{10}[T_{1/2}(yr)] = c_1 + c_2 \left(\frac{Z^2}{(1 - kI^2)A} \right) + c_3 \left(\frac{Z^2}{(1 - kI^2)A} \right)^2 + c_4 E_{\text{sh}} + h_i, \quad (19)$$

with $c_1 = 1174.353\,41$, $c_2 = -47.666\,855$, $c_3 = 0.471\,307$, $c_4 = 3.378\,848$, $k = 2.6$, and h_i is the blocking effect. Also, A and Z are the mass and charge number of the parent nuclei and I is the isospin effect with $I = (N-Z)/A$. E_{sh} is the shell correction energy taken from Moller *et al.* [59].

Another important factor that should be considered while calculating SF half-lives is mass inertia and hence a new formula is introduced by including the mass inertia parameter (I_{rigid}) and is given below:

$$\log_{10}[T_{1/2}(yr)] = c_1 + c_2 \left(\frac{Z^2}{(1 - kI^2)A} \right) + c_3 \left(\frac{Z^2}{(1 - kI^2)A} \right)^2 + c_4 E_{\text{sh}} + c_5 I_{\text{rigid}} + h_i. \quad (20)$$

The rigid body mass inertia of a nucleus [60,61] is given by $I_{\text{rigid}} = B_{\text{rigid}}[1 + 0.31\beta_2 + 0.44\beta_2^2 + ...]$ where the mass parameter, $B_{\text{rigid}} = \frac{2}{5}MR^2 = 0.0138A^{5/3}(\hbar^2/\text{MeV})$. Here M is mass of the nucleus, β_2 is the quadrupole deformation, and $R = 1.2A^{1/3}$(fm). The constants in the new equation are obtained by fitting it to the experimental SF half-lives. The constants are $c_1 = 1208.763\,104$, $c_2 = -49.264\,392\,88$, $c_3 = 0.486\,222\,575$, $c_4 = 3.557\,962\,857$, $c_5 = 0.042\,925\,714\,94$ with a fixed value of $k = 2.6$ [37] and h_i is the blocking effect for the unpaired nucleon. For even-even heavy and superheavy

nuclei $h_i = 0$, for odd N nuclei, $h_{eo} = 2.749\,814$, and for odd Z nuclei, $h_{oe} = 2.490\,760$.

In Table V, we made a comparison between experimental SF half-life, half-life using the equation by Bao *et al.* [37], and half-life using mass inertia dependent formula, for even-even heavy and superheavy nuclei, and Table VI shows the comparison for odd N (left) and odd Z (right) heavy and superheavy nuclei. The first column denotes parent nuclides. The logarithm of experimental SF half-life [62–64], SF half-life calculated by new mass inertia dependent formula, and using Bao *et al.* [37] are shown in the second, third, and fourth columns respectively. From Tables V and VI, it is evident that there is good agreement between experimental and theoretical half-life using new mass inertia dependent formula with an overall rms standard deviation for Tables V and VI is 1.772. The overall standard deviation using the formula by Bao *et al.* [37] is 1.841. Therefore it is clear that the inclusion of a mass inertia parameter could produce a better match with the experimental SF half-life. Significant deviation from experimental $T_{1/2}^{\text{SF}}$ occurs only for a few parent nuclei in Table VI like ^{249}Cf, ^{259}Fm, and ^{245}Md. As SF is a complex process compared to other decay modes, this significant deviation in $T_{1/2}^{\text{SF}}$ for few nuclei are acceptable. When we compare our predicted results with other theoretical models to calculate SF like HFB or SKM* [65–68], one will understand that the discrepancy from different theoretical models can be high orders of magnitude in the case of SF due to its complex nature. In our present work, to determine modes of decay, alpha decay half-life is calculated using the MGLDM and SF half-life computed using the equation by Bao *et al.* [37] and by the mass inertia dependent formula for SF.

If the concept of the island of stability is valid, then from experiments, we expect our newly synthesized SHN to emit a series of alpha particles gradually leaving the boundary of island and eventually undergo fission. For the isotope $^{291,293-295}$Og, decay modes and alpha decay half-lives, calculated using our model, predicted by Bao *et al.* [37], and experimentally detected values are shown in Table VII. Those SHN with $T_{1/2}^{\alpha} < T_{1/2}^{\text{SF}}$ will survive fission and undergo alpha decay and hence can be detected experimentally in laboratories. From Table VII, it is understood that, after each alpha decay, the $T_{1/2}^{\text{SF}}$ of the parent nucleus in a decay chain decreases

TABLE V. Comparison between experimental and theoretical spontaneous fission half-life (in years) of even-even heavy and superheavy nuclei.

Nucleus	$T_{1/2}^{SF}$			Nucleus	$T_{1/2}^{SF}$		
	Expt.	Present	Bao et al. [37]		Expt.	Present	Bao et al. [37]
^{232}Th	21.08	21.90	22.22	^{250}Fm	−0.10	−0.50	−0.67
^{234}U	16.18	15.57	16.04	^{252}Fm	2.10	0.67	0.89
^{236}U	16.4	16.08	16.26	^{254}Fm	−0.20	−0.92	−1.04
^{238}U	15.91	16.32	16.04	^{256}Fm	−3.48	−3.08	−3.71
^{236}Pu	9.18	9.04	9.65	^{252}No	−6.54	−5.35	−5.38
^{238}Pu	10.68	10.02	10.24	^{254}No	−3.04	−3.66	−3.28
^{240}Pu	11.06	10.94	10.84	^{256}No	−4.77	−4.79	−4.72
^{242}Pu	10.83	11.32	10.92	^{254}Rf	−12.10	−9.64	−9.35
^{244}Pu	10.82	11.69	11.08	^{256}Rf	−9.71	−7.46	−6.98
^{240}Cm	6.28	4.07	4.52	^{258}Rf	−9.35	−7.92	−7.74
^{242}Cm	6.85	5.55	5.34	^{260}Rf	−9.20	−8.63	−8.87
^{244}Cm	7.12	6.45	6.69	^{262}Rf	−7.18	−8.38	−8.32
^{246}Cm	7.26	7.41	7.35	^{258}Sg	−10.00	−10.03	−9.63
^{248}Cm	6.62	7.66	7.41	^{260}Sg	−9.65	−10.05	−9.8
^{250}Cm	4.05	5.38	4.61	^{262}Sg	−9.32	−10.27	−10.41
^{242}Cf	−1.33	−1.19	−1.17	^{264}Sg	−8.93	−9.47	−9.42
^{246}Cf	3.26	1.96	2.09	^{266}Sg	−7.86	−7.59	−7.48
^{248}Cf	4.51	3.46	3.27	^{264}Hs	−10.20	−11.96	−12.1
^{250}Cf	4.23	4.15	4.31	^{270}Ds	−8.60	−10.23	−10.22
^{252}Cf	1.93	2.06	2.11	^{282}Cn	−10.60	−11.28	−11.28
^{254}Cf	−0.78	−0.12	−0.82	^{284}Cn	−8.50	−9.37	−9.65
^{246}Fm	−6.6	−4.23	−4.15	^{286}Fl	−8.08	−5.82	−5.95

and finally reaches a low half-life where the spontaneous fission half-life becomes less than the alpha decay half-life and undergoes fission. We were able to successfully reproduce experimental alpha decay half-lives and decay chains in the case of ^{294}Og. Also, from Table VII it is clear that there is good agreement between predictions made by Bao et al. and our calculations in the case of ^{291}Og, ^{293}Og, and ^{294}Og. The pictorial representation of modes of decay of other isotopes of Og with mass numbers ranging from 290 to 296 is shown in Fig. 3. The calculated Q value and alpha decay half-life are also shown in the figure on the right side corresponding to each decay. Figure 3 depicts that most isotopes of Og, once synthesized, undergo continuous alpha decay and decays to various isotopes of Cn, which is extremely unstable and radioactive with a short half-life, and then spontaneous fission occurs. The complete information in a decay chain, like whether the decay is by alpha decay or spontaneous fission, and if alpha decay occurs, then the half-life, length of decay chain, and Q value in reactions, is all predicted through our model. We predict that the isotope Og with mass numbers 290, 292, 293, 294, and 296 decays by three alpha chains followed by spontaneous fission. ^{295}Og decays by four alpha chains

TABLE VI. Comparison between experimental and theoretical spontaneous fission half-lives (in years) for odd N (left) and odd Z (right) heavy and superheavy nuclei.

Nucleus	$T_{1/2}^{SF}$			Nucleus	$T_{1/2}^{SF}$		
	Expt.	Present	Bao et al. [37]		Expt.	Present	Bao et al. [37]
^{235}U	19.00	19.25	19.43	^{241}Am	14.08	11.41	11.36
^{239}Pu	15.90	13.96	14.02	^{243}Am	14.30	12.00	11.57
^{243}Cm	11.74	9.56	9.54	^{249}Bk	9.26	9.00	8.80
^{245}Cm	12.65	10.46	10.28	^{253}Es	5.80	3.50	3.67
^{237}Cf	−6.18	−4.84	−3.81	^{255}Es	3.41	1.33	0.81
^{249}Cf	10.9	7.49	6.91	^{245}Md	−10.54	−6.64	−6.63
^{255}Fm	4.00	1.27	0.99	^{247}Md	−8.20	−4.31	−3.99
^{257}Fm	2.12	−0.30	−0.99	^{259}Lr	−6.01	−4.28	−4.48
^{259}Fm	−7.32	−0.73	−1.24	^{261}Lr	−4.13	−4.17	−4.25
^{253}Rf	−11.82	−7.95	−7.83	^{255}Db	−6.60	−7.89	−7.49
^{255}Rf	−7.04	−5.00	−4.67	^{257}Db	−6.60	−5.49	−4.96
^{259}Rf	−5.88	−5.09	−5.06	^{263}Db	−5.82	−5.51	−5.44

TABLE VII. Modes of decay of isotopes $^{291,293-295}$Og and its comparison with experimental modes of decay and modes predicted by Bao *et al.* [37].

Parent nuclei	Q value (MeV)	$T_{1/2}^{SF}$(s) Present	$T_{1/2}^{\alpha}$(s) Present	$T_{1/2}^{\alpha}$(s) Expt.	Modes of decay Present	Modes of decay Expt.	Modes of decay Bao *et al.* [37]
^{291}Og	11.595	7.66×10^7	0.0016		α		α
^{287}Lv	10.995	1.96×10^6	0.0128		α		α
^{283}Fl	10.965	516.4944	0.0039		α		α
^{279}Cn	11.025	2.3×10^{-3}	0.7×10^{-3}		α/SF		α/SF
^{275}Ds	10.395	16.1103	0.0071		α		α
^{293}Og	11.915	6.08×10^8	2.69×10^{-4}		α		α
^{289}Lv	11.105	2.18×10^7	6.26×10^{-3}		α		α
^{285}Fl	10.555	2.10×10^4	4.16×10^{-2}		α		α
^{281}Cn	10.455	1.90×10^{-2}	1.88×10^{-2}		α /SF		SF
^{294}Og	11.835	1.44×10^5	3.95×10^{-4}	8.90×10^{-4}	α	α	α
^{290}Lv	11.005	2.17×10^4	10.7×10^{-3}	7.10×10^{-3}	α	α	α
^{286}Fl	10.365	48.2523	1.31×10^{-1}	2.60×10^{-1}	α	α/SF	α
^{282}Cn	10.175	9.65×10^{-4}	0.1039		SF	SF	SF
^{295}Og	11.695	8.54×10^9	0.81×10^{-3}		α		α
^{291}Lv	10.895	9.51×10^6	0.0198		α		α
^{287}Fl	10.155	5.72×10^5	0.4831		α		α
^{283}Cn	9.935	3.5484	0.4753		α		SF
^{279}Ds	10.085	0.0021	0.0417		SF		

followed by spontaneous fission. In most cases, the properties of the potential daughter nucleus or grand-daughter nucleus will be a known fact or could be studied experimentally, and hence the properties of unknown parent nucleus can be identified based on these predicted decay chains.

IV. CONCLUSION

In our present work, we have studied the feasibility for alpha and other cluster decay in the case of various isotopes of SHN Og ranging 288–296 via heavy cluster emission. We have calculated the half-life for all possible heavy cluster de-

cay in the framework of the MGLDM with Q value dependent preformation factor. The heavy clusters with half-lives comparable to or less than the alpha half-life which are probable for emission are identified. Thus our study supports the predictions of heavy cluster emission of clusters with $Z_C > 28$ from SHN with $Z > 110$ by Poenaru *et al.* [45,54,55]. We could be able to reproduce experimentally the measured alpha decay half-life and decay chain of ^{294}Og with good accuracy. Hence we use our model to predict the alpha decay half-life, decay chains, and decay modes of various isotopes of SHN Og. We expect that our present work will be an asset to study the properties of SHN and a guiding tool to conduct experiments on these isotopes in the near future.
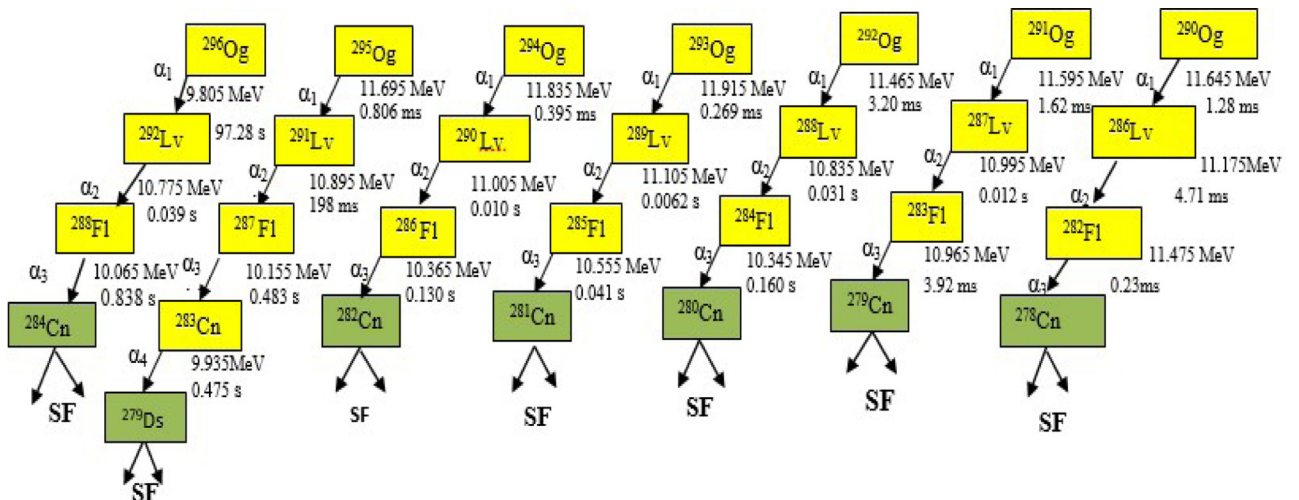

FIG. 3. Figure shows the modes of decay of various isotopes of Og.

[1] S. Hofmann and G. Munzenberg, Rev. Mod. Phys. **72**, 733 (2000).

[2] Yu. Ts. Oganessian, J. Phys. G: Nucl. Part. Phys. **34**, R165 (2007).

[3] Yu. Ts. Oganessian, V. K. Utyonkov, Yu. V. Lobanov, F. Sh. Abdullin, A. N. Polyakov, R. N. Sagaidak, I. V. Shirokovsky, Yu. S. Tsyganov, A. A. Voinov, A. N. Mezentsev, V. G. Subbotin, A. M. Sukhov, K. Subotic, V. I. Zagrebaev, S. N. Dmitriev, R. A. Henderson, K. J. Moody, J. M. Kenneally, J. H. Landrum, D. A. Shaughnessy *et al.*, Phys. Rev. C **79**, 024603 (2009).

[4] S. Hofman, S. Heinz N, R. Mann, J. Maurer, G. Münzenberg, S. Antalic, W. Barth, H. G. Burkhard, L. Dahl, K. Eberhardt, R. Grzywacz, J. H. Hamilton, R. A. Henderson, J. M. Kenneally, B. Kindler, I. Kojouharov, R. Lang, B. Lommel, K. Miernik, D. Miller *et al.*, Eur. Phys. J. A **52**, 180 (2016).

[5] H. Haba, Nat. Chem. **11**, 10 (2019).

[6] K. Siwek-Wilczyńska, T. Cap, M. Kowal, A. Sobiczewski, and J. Wilczyński, Phys. Rev. C **86**, 014611 (2012).

[7] Z. H. Liu and J.-D. Bao, Phys. Rev. C **80**, 054608 (2009).

[8] K. Siwek-Wilczyńska, T. Cap, and J. Wilczyński, Int. J. Mod. Phys. E **19**, 500 (2010).

[9] Z.-H. Liu and J.-D. Bao, Phys. Rev. C **83**, 044613 (2011).

[10] Z.-H. Liu and J.-D. Bao, Phys. Rev. C **84**, 031602(R) (2011).

[11] C. Wang, J. Zhang, Z. Z. Ren, and C. W. Shen, Phys. Rev. C **82**, 054605 (2010).

[12] C. Shen, G. Kosenko, and Y. Abe, Phys. Rev. C **66**, 061602(R) (2002).

[13] V. I. Zagrebaev, Phys. Rev. C **64**, 034606 (2001).

[14] V. I. Zagrebaev and W. Greiner, Phys. Rev. C **78**, 034610 (2008).

[15] G. G. Adamian, N. V. Antonenko, and W. Scheid, Nucl. Phys. A **618**, 176 (1997).

[16] A. S. Zubov, G. G. Adamian, and N. V. Antonenko, Phys. Part. Nucl. **40**, 847 (2009).

[17] A. Nasirov, K. Kim, G. Mandaglio, G. Giardina, A. Muminov, and Y. Kim, Eur. Phys. J. A **49**, 147 (2013).

[18] W. Li, N. Wang, J. F. Li, H. Xu, W. Zuo, E. Zhao, J. Q. Li, and W. Scheid, Europhys. Lett. **64**, 750 (2003).

[19] W. Li, N. Wang, F. Jia, H. Xu, W. Zuo, Q. Li, E. Zhao, J. Li, and W. Scheid, J. Phys. G: Nucl. Part. Phys. **32**, 1143 (2006).

[20] M. Huang, Z. Gan, X. Zhou, J. Li, and W. Scheid, Phys. Rev. C **82**, 044614 (2010).

[21] Z.-Q. Feng, G.-M. Jin, F. Fu, and J.-Q. Li, Nucl. Phys. A **771**, 50 (2006).

[22] Yu. Ts. Oganessian, V. K. Utyonkov, Yu. V. Lobanov, F. Sh. Abdullin, A. N. Polyakov, R. N. Sagaidak, I. V. Shirokovsky, Yu. S. Tsyganov, A. A. Voinov, G. G. Gulbekian *et al.*, Phys. Rev. C **74**, 044602 (2006).

[23] L. Stavsetra, K. E. Gregorich, J. Dvorak, P. A. Ellison, I. Dragojević, M. A. Garcia, and H. Nitsche, Phys. Rev. Lett. **103**, 132502 (2009).

[24] P. A. Ellison, K. E. Gregorich, J. S. Berryman, D. L. Bleuel, R. M. Clark, I. Dragojević, J. Dvorak, P. Fallon, C. Fineman-Sotomayor, J. M. Gates, O. R. Gothe, I. Y. Lee, W. D. Loveland, J. P. McLaughlin, S. Paschalis, M. Petri, J. Qian, L. Stavsetra, M. Wiedeking, and H. Nitsche, Phys. Rev. Lett. **105**, 182701 (2010).

[25] A. Sobiczewski, Phys. Rev. C **94**, 051302(R) (2016).

[26] M. Sayahi, V. Dehghani, D. Naderi, and S. A. Alavi, Z. Naturforsch. A **74**, 551 (2019).

[27] X. J. Bao, S. Q. Guo, H. F. Zhang, and J. Q. Li, Phys. Rev. C **95**, 034323 (2017).

[28] M. Ismail and A. Adel, Phys. Rev. C **97**, 044301 (2018).

[29] G. Gamow, Z. Phys. **51**, 204 (1928).

[30] R. W. Gurney and E. U. Condon, Nature (London) **122**, 439 (1928).

[31] D. N. Poenaru, M. Ivascu, A. Sandulescu, and W. Greiner, Phys. Rev. C **32**, 572 (1985).

[32] B. Buck, A. C. Merchant, and S. M. Perez, Phys. Rev. C **45**, 2247 (1992).

[33] H. F. Zhang and G. Royer, Phys. Rev. C **76**, 047304 (2007).

[34] V. Yu. Denisov and A. A. Khudenko, At. Data Nucl. Data Tables **95**, 815 (2009).

[35] K. P. Santhosh and C. Nithya, Phys. Rev. C **97**, 064616 (2018).

[36] N. Bohr and J. A. Wheeler, Phys. Rev. **56**, 426 (1939).

[37] X. J. Bao, S. Q. Guo, H. F. Zhang, Y. Z. Xing, J. M. Dong, and J. Q. Li, J. Phys. G: Nucl. Part. Phys. **42**, 085101 (2015).

[38] J. Blocki, J. Randrup, W. J. Swiatecki, and C. F. Tsang, Ann. Phys. (N.Y.) **105**, 427 (1977).

[39] J. Blocki and W. J. Swiatecki, Ann. Phys. (N.Y.) **132**, 53 (1981).

[40] G. Royer and B. J. Remaud, J. Phys. G: Nucl. Part. Phys. **10**, 1057 (1984).

[41] G. Royer and B. Remaud, Nucl. Phys. A **444**, 477 (1985).

[42] M. Wang, G. Audi, F. G. Kondev, W. J. Huang, S. Naimi, and X. Xu, Chin. Phys. C **41**, 030003 (2017).

[43] H. Koura, T. Tachibana, M. Uno, and M. Yamada, Prog. Theor. Phys. **113**, 305 (2005).

[44] P. B. Price, R. Bonetti, A. Guglielmetti, C. Chiesa, R. Matheoud, C. Migliorino, and K. J. Moody, Phys. Rev. C **46**, 1939 (1992).

[45] D. N. Poenaru, H. Stöcker, and R. A. Gherghescu, Eur. Phys. J. A **54**, 14 (2018).

[46] T. A. Jose and K. P. Santhosh, Ind. J. Pure Appl. Phys. **58**, 415 (2020).

[47] R. Bonetti and A. Guglielmetti, in *Heavy Elements and Related New Phenomena*, edited by R. K. Gupta and W. Greiner (World Scientific, Singapore, 1999), Vol. 2, p. 643.

[48] R. Bonetti and A. Guglielmetti, Rom. Rep. Phys. **59**, 301 (2007).

[49] H. J. Rose and G. A. Jones, Nature (London) **307**, 245 (1984).

[50] V. E. Viola Jr. and G. T. Seaborg, J. Inorg. Nucl. Chem. **28**, 741 (1966).

[51] A. Sobiczewski, Z. Patyk, and S. Cwiok, Phys. Lett. B **224**, 1 (1989).

[52] C. Qi, F. R. Xu, R. J. Liotta, and R. Wyss, Phys. Rev. Lett. **103**, 072501 (2009).

[53] D. N. Poenaru and W. Greiner, Phys. Scr. **44**, 427 (1991).

[54] A. I. Budaca, R. Budaca, and I. Silisteanu, Nucl. Phys. A **951**, 60 (2016).

[55] D. N. Poenaru, R. A. Gherghescu, and N. Carjan, Europhys. Lett. **77**, 62001 (2007).

[56] G. Royer, J. Phys. G: Nucl. Part. Phys. **26**, 1149 (2000).

[57] D. N. Poenaru, R. A. Gherghescu, and W. Greiner, Phys. Rev. Lett. **107**, 062503 (2011).

[58] D. N. Poenaru, R. A. Gherghescu, and W. Greiner, Phys. Rev. C **85**, 034615 (2012).

[59] P. Möller, A. J. Sierk, T. Ichikawa, and H. Sagawa, At. Data Nucl. Data Tables **109**, 1 (2016).

[60] A. Bohr and B. R. Mottelson, Dan. Mat. Fys. Medd. **30**, 1 (1955).

[61] J. M. Allmond and J. L. Wood, Phys. Lett. B **767**, 226 (2017).

[62] C. Xu and Z. Ren, Phys. Rev. C **71**, 014309 (2005).

[63] C. Xu, Z. Ren, and Y. Guo, Phys. Rev. C **78**, 044329 (2008).

[64] N. E. Holden and D. C. Hoffman, Pure Appl. Chem. **72**, 1525 (2000).

[65] R. Smolánczuk, J. Skalski, and A. Sobiczewski, Phys. Rev. C **52**, 1871 (1995).

[66] R. Smolánczuk, Phys. Rev. C **56**, 812 (1997).

[67] M. Warda and J. L. Egido, Phys. Rev. C **86**, 014322 (2012).

[68] A. Staszczak, A. Baran, and W. Nazarewicz, Phys. Rev. C **87**, 024320 (2013).